DEVELOPMENT AND APPLICATION OF COPPER-IMPREGNATED OIL PALM FIBRE ASH AS ADSORBENT FOR CYANIDE

***[1]Ajayi, O.A., [1]Olakunle, M.S., [1]Edet, M.O., [1]Dabai, F.N. and [2]Eletta, O.A.A.**

[1]Department of Chemical Engineering,
Ahmadu Bello University, Zaria. Kaduna state

[2]Department of Chemical Engineering,
University of Ilorin, Ilorin. Kwara state

*Corresponding author: aoajayi@abu.edu.ng and segeaj@gmail.com +2348033175209

ABSTRACT

Palm Kernel Fiber Ash (PKFA) was prepared via wet beneficiation, carbonization, and calcination at 700^{0}C for 6hrs. The PKFA was wet impregnated with Cu(NO_3) and calcined at 450^{0}C for 3hrs. The adsorbent formed was employed in cyanide removal from simulated wastewater. X-ray Fluorescence (XRF), X-ray Diffratograph (XRD), Fourier Transform Infra-red (FTIR) and Scanning Electron Microscope (SEM) were used to characterize the raw PKF, PKFA and calcined cupper impregnated PKF, while UV spectrophotometer was used to monitor the cyanide concentration. Batch adsorption experiments were carried out using 25 ml each of 25 ppm to 60 ppm cyanide solutions at different contact times, temperatures and adsorbent dosages. To establish optimum adsorption conditions, numerical optimization approach of Box-Behnken in Response Surface Methodology (RSM) was employed using the time, concentration, temperature and adsorbent dosages as variables at a fixed pH of 7. Adsorption efficiency of 85.27% was obtained with 47.39 ppm, adsorbent dosage of 2.82 g at 42 minutes contact time and temperature of 40^{o}C, having a desirability of 0.937. R^2 of 0.8461 obtained gave an indication of a very good correlation between the data points. The results indicated that Cu-PKFA can serve as a good sustainable adsorbent for cyanide in wastewater.

1.0 INTRODUCTION

Cassava (*Manihot esculenta Crantz*) processing wastewater effluent in the rural settings in Nigeria are indiscriminately discharged into the environment or public sewers thereby polluting the soil and invariably presenting a risk for the environment because of its cyanogen content. Cassava has a high level of toxicity as it contains large amounts of two cyanogenic glucosides, linamarin (96%) and lotaustralin (4%) (Szabo *et al.,* 2010). The hydrolysis or cyanogenesis of linamarin as well as other cyanogenic glucosides releases hydrogen cyanide (HCN). The indiscriminate discharge activities of the wastewater effluents reduce the quality of the shallow 'well water' and render it less suitable for human consumption. Wastewater from these processes that contains even trace amounts of cyanide must be treated before discharge into sewage systems because, cyanide toxicity presents a direct human hazard. Presence of cyanide in these wastewaters has the potential of poisoning drinking water when it infiltrates into the ground and renders the soil unproductive because of its acidic nature. The toxicity of cyanide is dependent upon the form in which it occurs. However, the cyanide anion CN^- is the primary toxic agent, regardless of origin (Ebbs, 2004).

A number of treatment processes based on natural degradation, chemical and biological oxidation, complexing, precipitation and recovery have been studied in the past for the removal of cyanides from waste water (Yeddou *et al*.,2010; Abbas *et al.,* 2014; Dash *et al.,*2009). Chemical methods such as ozonization, chemical oxidation, wet-air oxidation etc. have also been used for the treatment of effluent containing cyanide (Pueyo *et al*., 2016; Abdel-Aziz *et al.,* 2016). However, the use of expensive and hazardous chemicals (as reagents) and generation of huge amount of chemical sludge are the major constraints associated with these methods. Another method which is very commonly used for treating free or simple cyanide is alkaline chlorination (Mert *et al.,* 2014). But in this process, highly toxic intermediates like cyanogen's chloride are formed which creates additional environmental and health problems. Compared to the above methods, removal of cyanide can easily be achieved by adsorption. Soils, wastes and ores containing minerals such as ilmenite ($FeTiO_3$), hematite (Fe_2O3), bauxite [$AlO.OH/Al(OH)_3$] and pyrite (FeS_2), as well as mineral-groups such as feldspars, zeolites and clays have shown to effectively adsorb free and metal complexed cyanides (Zhang and Hendrix, 1991). Depending on the mineral, cyanide adsorption is usually a combination of two mechanisms: ion exchange, precipitation or

coulombic interaction. Cyanide attenuation by such mineral commodities purifies ground and surface waters but increases cyanide consumption in leaching operations. A wide range of organic and inorganic adsorbents such as agricultural by-products (Adams, 1994), pyrophyllite (Saxena *et al.,* 2001), plain and biological activated carbon (Dash *et al.,* 2009), synthetic activated carbon produced from porous sulfonated styrene/di-vinyl benzene resin (Oliver *et al.,* 2005) have been studied in the past.

The oil palm industry has been recognized for its contribution towards economic growth and rapid development; it has also contributed to environmental pollution due to the production of huge quantities of by-products from the oil extraction process (Parveen *et al.,* 2010). The waste products from oil palm processing consist of oil palm trunks (OPT), oil palm fronds (OPF), empty fruit bunches (EFB), palm pressed fibres (PPF), palm kernel shells, palm kernel cake and liquid discharge palm oil mill effluent (POME) (Singh *et al.,* 2010). According to Prasertsan and Prasertsan (1996), during processing in the palm oil mill more than 70% (by weight) of the processed fresh fruit bunch (FFB) was left over as oil palm waste. According to Herawan *et al.* (2013), two major solid wastes are generated during palm oil processing, which include, the extracted flesh fibre (mesocarp) and seed shell (endocarp). Preparation of adsorbents from agricultural by products has been given serious attention due to the growing interest in low cost adsorbent from renewable biomass, especially for applications concerning treatment of drinking water and wastewater (Castro *et al.,* 2000).

The palm oil tree (*Elaeis guineensis*) is a native of the humid tropics of West Africa. It is one of the major oil crops in the world, producing more oil than all other plants oil (Adeoluwa and Adeoye, 2008). During oil palm processing, about 20-24% of fresh fruit bunch (FFB) are converted to oil (Poku, 2002), while the remaining 76-80% are essentially waste-products. Anyanwu (2013) carried out a survey which revealed that on an average, Nigeria generates nothing less than 344,250 dry tonnes of empty fruit bunch (EFB), 382,500 dry tonnes of palm pressed fiber (PPF), 246,500 dry tonnes of palm shell (PS) and 633,250 dry tonnes of palm oil mill effluent (POME). This finding was corroborated by the report of Ohimain *et al*. (2013). Oil-palm shell and their fibre are good candidate for advanced material production, because they are available as wastes, which could be gotten free in small quantity or low price in huge quantity (Herawan *et al.,* 2013). Accordingly, this work reports on the development and application of Cu-PKFA as effective adsorbent for cyanide, while investigating the removal efficiency using graphical optimization technique in Box-Beknhen method.

2.0 METHODOLOGY

2.1 Sample Collection, Preparation and Impregnation with Copper (II) Nitrate

The oil palm fibre was collected from a traditional palm oil industry in Esit-Eket Local Government Area in Akwa Ibom State, Nigeria, having latitude of $4^{0}38'32$N, longitude-$7^{0}55'28$E at an altitude of 830 feet above sea level. The fibre collected was deoiled by soaking in hot deionized water and detergent for 24 hours. It was rinsed thoroughly in hot deionized water to remove all debris and then air dried. The air-dried oil palm fibre was carbonized for 72 hours in a rotary kiln (Asadpour *et al*., 2016). The resulting ash was washed in water, filtered, sieved to size of 250microns and subsequently left to settle for a day in quiescent condition. The settled ash was oven dried at 80°C for 6hours and ball milled to powdered form. Ashing of the palm kernel fiber was done in a muffle furnace at 550°C overnight followed by a further 1hr of heating at 750°C. The proximate analysis for the palm kernel fiber was conducted as detailed in ASTM E871, ASTMD1102 and ASTM E872.

The anchoring of copper on the palm kernel fiber ash was done using wet method of impregnation. 5 g of copper (II) nitrate was dissolved in 480ml of deionized water to form solution. 50 g of ash was weighed into a plastic sample holder which was then introduced into the copper (II) nitrate solution and stirred for 2 hrs. The resulting slurry was aged for 24 hrs before it was oven dried at 80ºC for 6 hrs and later calcined at 450ºC. Characterization at all stages of transformation was done using XRF, XRD, SEM and FTIR.

2.2 Preparation of the Cyanide Standard Solution

A stock solution of 1 g/L potassium cyanide (KCN) was prepared by dissolving 1g of KCN in 1000 ml of deionized water. Different concentrations of the cyanide from 10ppm to 60 ppm in steps of 10 ppm were prepared from the 1g/L KCN stock solution by serial dilution. Calibration linearity curve was generated using the five-prepared solution including a blank using Perkin Elmer LAMBDA XLS spectrophotometer with single beam sample compartment set at 575 nm. The linear Beer– Lambert relationship between absorbance and cyanide concentration for the calibration curve was established by plotting these parameters and observing the regression. The model

developed was useful for subsequent determination of unknown cyanide concentrations.

2.3 Experimental Procedure and Optimization Studies

Batch adsorption experiment was conducted by contacting copper impregnated adsorbent (1 g, 3 g, 5 g,) each with 25 ml solution (25 ppm, 42.5 ppm, 60 ppm, KCN) at time (6 min, 24 min, 42 min) and also at temperature (30^{o}C, 35^{o}C, 40^{o}C) in a 100 ml batch reactor at a stirring speed of 350 rpm. The concentration of cyanide after adsorption was determined using UV spectrophotometer. The adsorption efficiency or cyanide removal percentage was calculated using:

$$R(\%) = \frac{C_o - C}{C_o} \times 100 \quad (1)$$

Where R-Removal Efficiency, %

C_0-Initial Concentration of Cyanide, ppm

C-Final Concentration of Cyanide, ppm

The appropriate combination of optimum conditions for maximum adsorption of cyanide by Cu-PKFA was determined by means of a four-factor, three-level Box–Behnken experimental design combining with response surface modeling. As the initial step of RSM, a suitable approximation is introduced to find true relationship between the dependent variable (response) and the set of independent variables (factors). If knowledge concerning the shape of true response surface is insufficient, the preliminary model (generally a first-order model) is upgraded by introducing the second-order response surface design which is rotatable, meaning that the variance of the predicted response is the same at all points. (Paul, 2004), Rotatability is a reasonable basis for the selection of response surface design (Refaat, 2002). Because the purpose of response surface methodology (RSM) is optimization and as the location of the optimum is unknown prior to running the experiment, it makes sense to use design that provides equal precisions of estimation in all directions (Yetilmezsoy *et al.,* 2009). This work focuses on the design of four factors (initial concentration of cyanide, contact time, adsorbent dosage and temperature) to determine the optimum adsorption conditions, using percentage cyanide removal as response, as depicted in Table 1.

Table 1: Experimental Design Matrix with Response.

Std	Run	Factor 1 A: Temperature (degree C)	Factor 2 B: Time (mins)	Factor 3 C: Dosage (g)	Factor 4 D: Initial Conc.(ppm)	Response 1 Removal Efficiency (%)
3	1	30	42	3	42.5	88.45
27	2	35	24	3	42.5	78.69
8	3	35	24	5	60	75.21
7	4	35	24	1	60	76.87
11	5	30	24	3	60	72.41
1	6	30	6	3	42.5	78.96
12	7	40	24	3	60	83.76
19	8	30	24	5	42.5	75.98
6	9	35	24	5	25	76.79
13	10	35	6	1	42.5	78.32
18	11	40	24	1	42.5	82.56
2	12	40	6	3	42.5	84.34
21	13	35	6	3	25	76.59
9	14	30	24	3	25	83.12
25	15	35	24	3	42.5	77.98
16	16	35	42	5	42.5	79.29

20	17	40	24	5	42.5	83.98
15	18	35	6	5	42.5	73.94
17	19	30	24	1	42.5	80.32
14	20	35	42	1	42.5	81.33
4	21	40	42	3	42.5	84.87
23	22	35	6	3	60	74.91
29	23	35	24	3	42.5	83.34
26	24	35	24	3	42.5	79.87
5	25	35	24	1	25	81.44
24	26	35	42	3	60	78.99
28	27	35	24	3	42.5	77.69
22	28	35	42	3	25	78.98
10	29	40	24	3	25	82.12

Table 2: Proximate analysis from XRF (wt%)

Property	Moisture content	Volatile matter	Crude fiber	Ash	Crude protein	Carbohydrate
Value	7.21	43.78	13.97	3.16	12.67	10.21

Table 3: Elemental analysis for various forms of palm

Oxide	RPKF	PKFA	Cu-PKFA
SiO_2	43.6	66.5	61.7
Al_2O_3	11.4	6.8	5.4
Fe_2O_3	8.4	5.9	6.1
CaO	4.8	5.3	4.3
MgO	3.5	3.1	2.6
SO_3	0.5	1.2	0.7
K_2O	3.6	4.9	3.6
Na_2O	1.7	2.8	1.9
C	21.5	2.6	0.6
Cu	0.4	0.1	7.8

RPKF *Raw Palm Kernel Fiber*
PKFA *Palm Kernel Fiber Ash*
Cu-PKFA *Copper-impregnated Palm*

3.0 RESULTS AND DISCUSSION

3.1 Characterization of Raw Material and Biosorbent

Proximate analysis of raw PKF and XRF for raw, ash and Cu-impregnated PKF

The proximate analysis result obtained are tabulated in Table 2, which was found to compare favorably with the literature (Shariff *et al.,* 2014 and Abdullah *et al.,*2011).
The elemental composition showed in Table 3 points to over 40% (weight basis) richness in silicon oxide and about 21.5% carbon content. This observation tends to conform with the work reported by Zarina *et al.* (2013).

Upon thermal treatment, the silica content tends to increase proportionately with decrease in carbon content. This might have resulted from the carbonization process in which the inherent carbon was oxidized to carbon dioxide or carbon monoxide. Ironically, such compound cannot be detected by the XRF analysis adopted in this work. The residual carbon in the ash material is an indication of incomplete combustion, which was further improved during calcination. The successful impregnation of copper on palm kernel ash was

confirmed from the increased in the copper content observed in the elemental composition, which led to decrease of other oxides in the fiber ash.

XRD analysis of PKFA ash and Cu-impregnated PKFA

The XRD pattern for the ash, showed the major phases of the palm kernel ash to be α-quartz (SiO_2) which tend to corroborate with the XRF result and work reported by Yojiro and Ayaaki (1990). Another noticeable phase is crystobalite, as depicted in Figure 1. The Copper impregnated ash tends to retain the phases present in the ash with the copper undetected by the XRD due to its low weight percentage. The reduced species (Cu^+ and CuO) could be produced by the reducing action of the carbon surface during the thermal treatment at high temperatures. The peak at around 2 theta values of 39 and 49 were observed to change due to the presence of copper on palm kernel fiber ash.

Scanning Electron Microscope (SEM) Analysis of raw PKF, ash and Cu-impregnated PKF

The SEM in Figure 2a reveals the heterogeneous structure of RPKA, with lacuna deposited on pores through which natural mass transfer processes take place (Chua *et al*., 2009). The whitish material could be of silica in nature conforming to similar observation by Shinoj *et al*. (2011), who claimed that silica bodies are found to be spread at the entire fiber surface. Figure 2b shows the morphology of PKFA having a relatively smooth solid structure mainly voids of pores. The heat effect on RPKF could be noticed by the waxy cuticle layer with more defined pores. The roughness of PKFA is known to enhance the mechanical interlocking at the surface and reactivity.

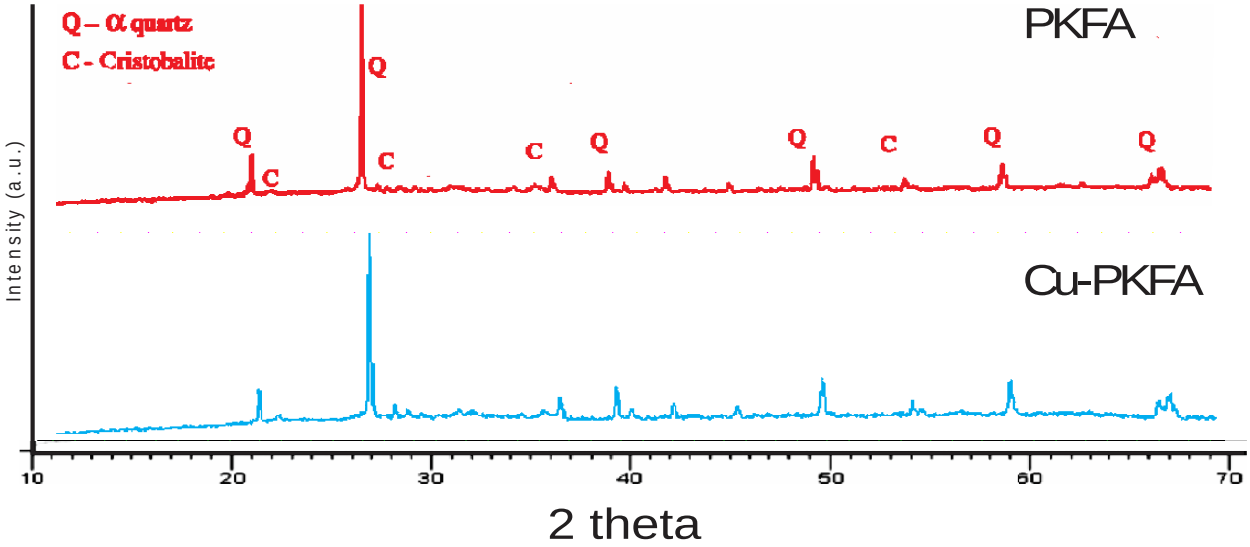

Figure 1. XRD patterns for raw and calcined-impregnated palm kernel

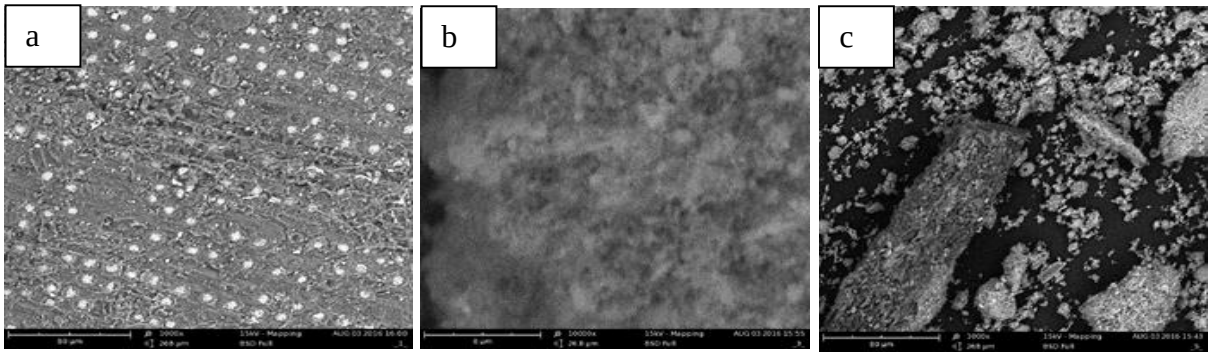

Figure 2. SEM images for: (a) PKF (b) PKFA (c) Cu-PKFA

SEM image of Figure 2c reflects the morphological changes, resulting from the introduction of copper oxide. The dispersed nature and almost even distribution might have resulted from copper impregnation inside the porous structure. Some part of the ash was observed to be unaffected (see the big agglomerate) properly due to mass transfer resistance, *viz-a-viz* challenges in mixing. This was found to conform to the works reported by Depci (2011).

Fourier Transform Infra-Red Spectra (FTIR) Analysis of raw PKF, ash and Cu-impregnated PKF

The FTIR was used to detect the presence of functional group in RPKA, PKFA and Cu-PKFA, as depicted in Figures 3(a-c), respectively. Figures 3a shows bands at 628.81 and 623.18cm^{-1} attributed to C-H alkenes out-of-plane bend. Vibrational bands at 1643.41 cm^{-1} reveals the presence of C=C of amide functional group; while that at 2353.83 cm^{-1} indicates the presence of (C-H) alkanes stretch. Vibrational bands at 3427.62 cm^{-1} reveals the presence of Si-O functional group. The shift or disappearance and emergence of bands may be due to the formation of chemical bond between functional groups present on the newly formed materials, which agrees with the report of Ridzuan *et al.,* (2014). On the basis of the FTIR, confirmation of potential application for adsorption can be deduced with good removal efficiency.

Figure 3b had bands at 1041.6 cm^{-1} and 1107 cm^{-1} which are attributed to C-C functional groups. Peak 1643.41 cm^{-1} identifies the presence of C=C functional group of amides, not affected by heat treatment. Appearance of vibrational bands at 1041.00 and 461.03 cm^{-1} corresponding to the bending and out-of-plane deformation of Si-O bonds, respectively. The position and shape of bands at 1041 and 3433.41cm^{-1} imply a stoichiometric silicon dioxide (Hamelmann *et al*, 2005).

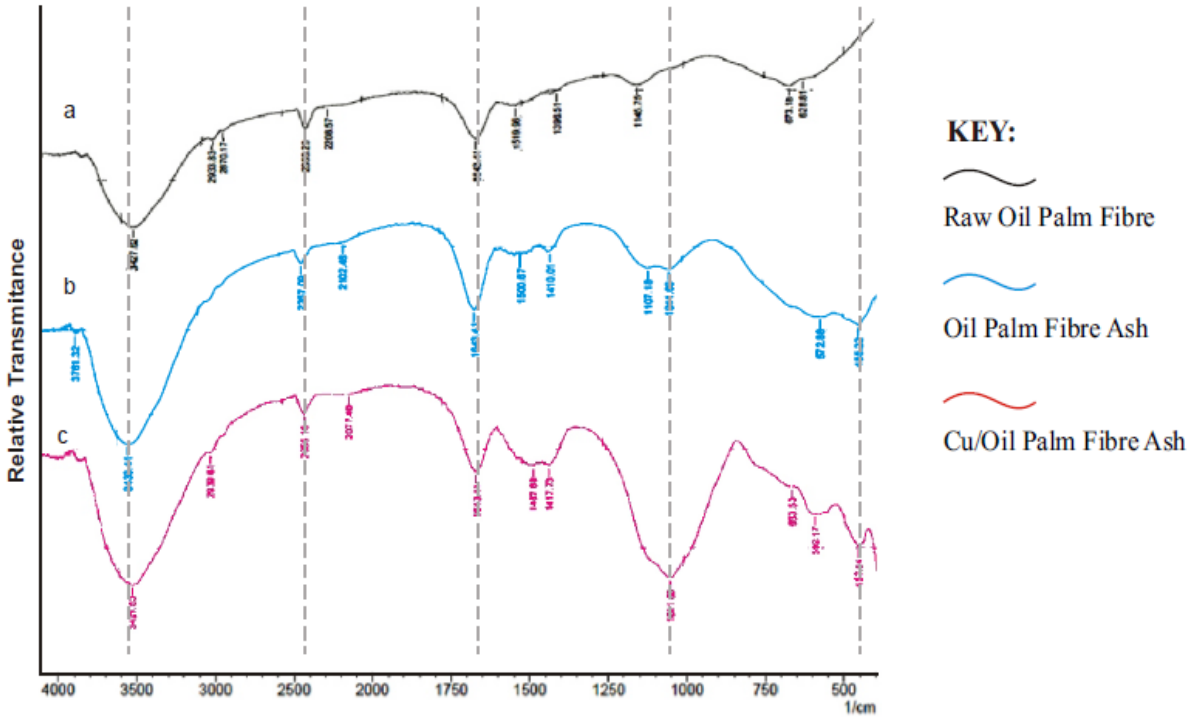

Figure 3. FTIR result for: (a) Raw (b) Carbonised and (c) Copper-Impregnated Palm Fibre.

Figure 3c had band at 1041.6 cm^{-1} indicates the presence of C-X fluoride functional group as well as the Si-O bond. There were clear band shifts and intensity decreased of band at 592.17 cm^{-1}, 663.53 cm^{-1}, 1467.88 cm^{-1}, 2077.40 cm^{-1}, 2939.61 cm^{-1} and 3421.83 cm^{-1}, mainly blamed on the impregnation effect of copper. The shift in the last band mentioned was attributed to formation of silanol (Si-OH) functional group, needed for accommodating incoming copper oxide, since Si-O bonds are rather too strong.

3.2 Box-Behnken Analysis

Regression Analysis of Batch Adsorption Experimental Data

The experiments were conducted according to Box-Behnken design as shown in Table 3 in order to search for the optimum combination of investigated parameters for cyanide removal. It was observed that the removal efficiency was influenced by the individual and combined effects of the factors considered.

An empirical relationship between the response and input variables in coded terms is expressed by the following response surface reduced quadratic model equation 2:

$$\text{Removal Efficiency} = +79.51 + 1.87*A + 2.07*B - 1.30*C - 1.41*D + 3.12*A^2 + 0.38*B^2 - 1.23*C^2 - 1.84*D^2 - 2.24*A*B + 1.44*A*C + 3.09*A*D + 0.59*B*C + 0.42*B*D + 0.75*C*D \quad (2)$$

Equation 2 revealed how the individual variables or double interactions affected cyanide removal. Negative coefficient values indicate that individual or double interaction factors negatively affect biosorption (*i.e.*, removal percentage decreases), whereas positive coefficient values mean that factors increase cyanide removal in the tested range.

Adequacy of the selected model

Linear, two-factor interaction (2FI), quadratic and cubic models were used to analyze the experimental data in order to obtain the appropriate regression equations as shown in Table 4. It can be seen that p values for quadratic model was lower than 0.01 and Design Expert 8.0 suggested the model to be significant. As a natural log transformation was applied to the experimental data, the interaction of two factors (2FI) and the linear model was suggested to be insignificant using the response surface methodology. The cubic model was assigned as aliased. From the model summary statistics, it can be seen that the ''R^2'' of 0.8461 was in reasonable agreement with the ''Adjusted R^2'' of 0.6921 for the quadratic model. The "Pred R-Squared" of 0.3432 is not as close to the "Adj R-Squared" of 0.6921 as one might normally expect. This may indicate a large block effect or a possible problem with your model and/or data. Things to consider are model reduction, response tranformation, outliers, etc. Accordingly, the results indicate that the quadratic model provide an excellent explanation for the relationship between the independent variables and the corresponding response.

Table 4: Selection of Satistisfactory Model - Sequential Model Sum of Squares

Source	Sum of Squares	DF	Mean Square	F Value	Prob > F	Remark
Mean	1.842E+005	1	1.842E+005			
Linear	137.42	4	34.35	3.32	0.0267	
2FI	70.81	6	11.80	1.20	0.3523	
Quadratic	118.16	4	29.54	6.96	0.0026	Suggested
Cubic	22.53	8	2.82	0.46	0.8480	Aliased
Residual	36.85	6	6.14			
Total	1.846E+005	29	6364.29			

ANOVA for response surface quadratic model

Table 5 shows the ANOVA analysis of the cyanide removal which influenced the model development. The larger the value of F and the smaller the value of p, the more significant is the corresponding coefficient term (Kalavathy *et al.,* 2009). The value of p was lower than 0.05, indicating that the model may be considered to be statistically significant. For the removal of cyanide by pretreated copper-dosed palm kernel fiber adsorbent, the F and p values for the ANOVA results (Table 5) indicated that the model is significant. In this study, A, B, C, D, A^2, D^2, AB, AD are significant model terms. The other model terms whose p values are listed as being greater than 0.1000 in Table 5 are not significant factors.

If there are many insignificant model terms (not counting those required to support hierarchy), model reduction may improve your model. The "Lack of Fit F-value" of 0.72 implies the Lack of Fit is not significant relative to the pure error. There is a 69.16 % chance that a "Lack of Fit F-value" this large could occur due to noise. Non-significant lack of fit is good -- we want the model to fit.

Table 5: Analysis of Variance

Source	Sum of Squares	DF	Mean Square	F Value	Prob > F	
Model	326.39	14	23.31	5.50	0.0015	*significant*
A-Temperature (^{0}C)	*41.78*	*1*	*41.78*	*9.85*	*0.0073*	*significant*
B-Time (min)	*51.46*	*1*	*51.46*	*12.13*	*0.0037*	*significant*
C-Dosage (mg/l)	*20.41*	*1*	*20.41*	*4.81*	*0.0456*	*significant*
D-Init. Conc of CN (ppm)	*23.77*	*1*	*23.77*	*5.60*	*0.0329*	*significant*
A^2	*63.20*	*1*	*63.20*	*14.90*	*0.0017*	*significant*
B^2	*0.96*	*1*	*0.96*	*0.23*	*0.6424*	*not significant*
C^2	*9.87*	*1*	*9.87*	*2.33*	*0.1494*	*not significant*
D^2	*21.93*	*1*	*21.93*	*5.17*	*0.0393*	*significant*
AB	*20.07*	*1*	*20.07*	*4.73*	*0.0472*	*significant*
AC	*8.29*	*1*	*8.29*	*1.96*	*0.1838*	*not significant*
AD	*38.13*	*1*	*38.13*	*8.99*	*0.0096*	*significant*
BC	*1.37*	*1*	*1.37*	*0.32*	*0.5790*	*not significant*
BD	*0.71*	*1*	*0.71*	*0.17*	*0.6878*	*not significant*
CD	*2.24*	*1*	*2.24*	*0.53*	*0.4799*	*not significant*
Residual	59.38	14	4.24			
Lack of Fit	*38.26*	*10*	*3.83*	*0.72*	*0.6916*	*not significant*
Pure Error	*21.12*	*4*	*5.28*			
Cor Total	385.78	28				

Eliminating these insignificant model terms from Equation 1 we have;

Cyanide Removal Efficiency= +79.51 +1.87*A +2.07*B-1.30*C-1.41*D+3.12*A^2-1.84*D^2-2.24*A*B +3.09*A*D (2)

Diagnostic plots

Data are analysis was done to check the normal probability plot and a dot diagram of residuals correlation as shown in Figure 4a. The data points on this plot lie reasonably close to a straight line, lending support to the conclusion that A, D, A^2 and D^2 were highly significant effects, while C, D, AB and AD were significant effects and that the underlying assumptions of the analysis were satisfied.

The data are also analyzed to check the correlation between the experimental and predicted percentage removal, as shown in Figure 4b. The experimental values were the result obtained, while the predicted values were obtained by calculation from the quadratic equation. It is shown in Figure 4b that the data points on the plot are distributed almost near to the straight line, indicating a good relationship between the experimental and predicted values of the response. This observation is suggestive that the selected quadratic model might be adequate in predicting the response variables for the experimental data.

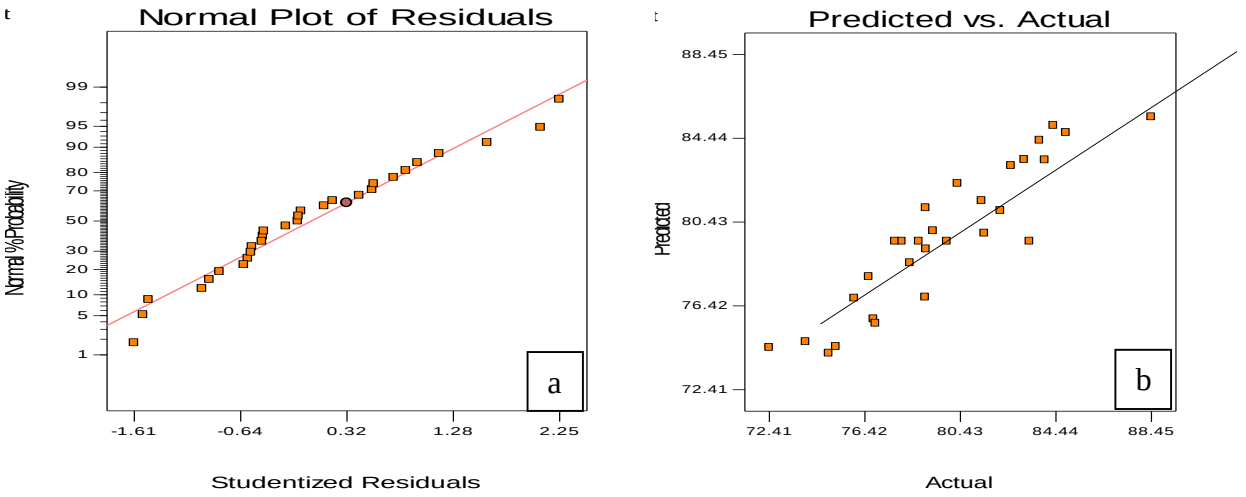

Figure 4: (a) Normal plot of residual **(b) Predicted vs Actual or Experimental**

Response surface contour plot

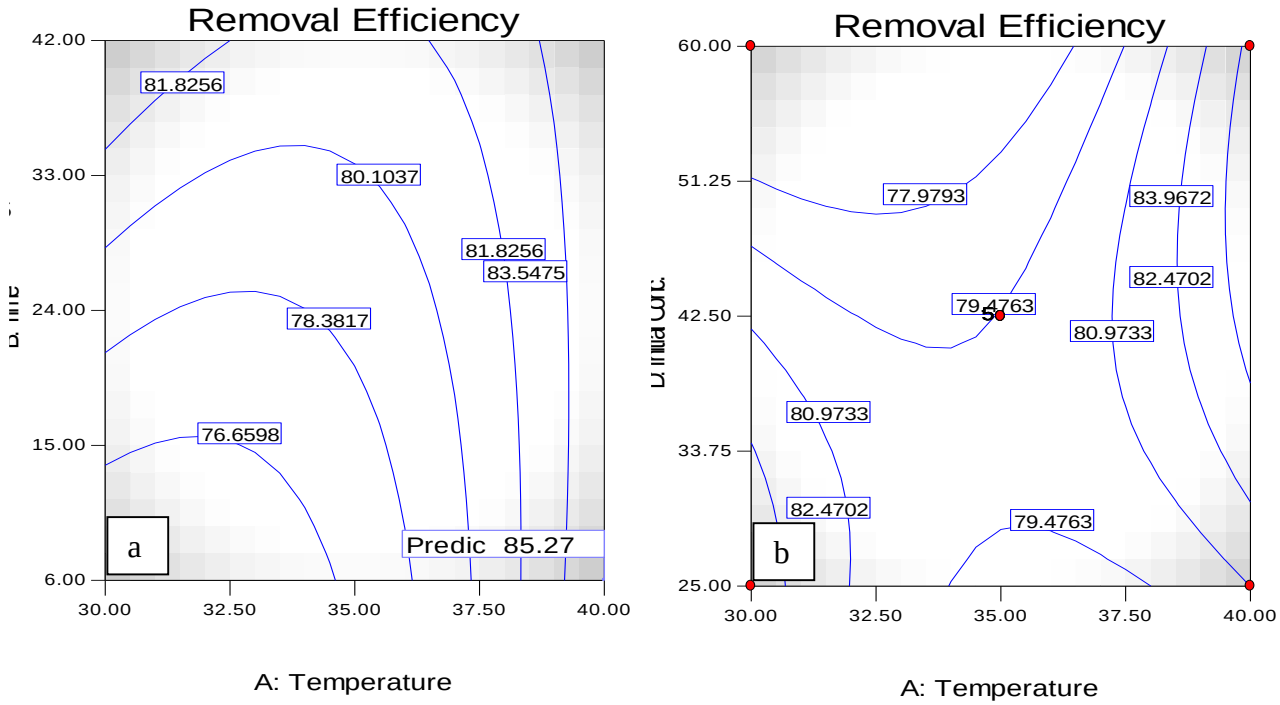

Figure 5. Response surface contour (a) Temp. vs Time (b) Temp. vs Initial Concentration

The response surface contour plots of percentage removal of cyanide versus the interactive effect of temperature, contact time and initial cyanide concentration are shown in Figures 5 a and b. Each contour plot represents a number of combinations of two test variables with the other variable maintained at zero levels. The maximum percentage removal of cyanide could be noticed by the surface confined in the smallest curve (circular or elliptical) of the contour plot. This observation was seen for the interactive effect of temperature and time, which increased in their values resulted in higher removal efficiency. The temperature-initial concentration interactive effects showed a hilly contour nature, where the maximum percentage converges at the top of the so called 'hill'.

The studies of the contour plots reveal the range for the best optimal values of the process conditions, which are temperature 37-40^{0}C, contact time 33-42 min and initial cyanide concentration 42.5–60 ppm which agrees with the batch adsorption studies investigated earlier.

Optimization of Cyanide Removal

Table 6: Numerical Optimization for Cyanide Removal

Constraints							
Name	***Goal***	***Lower Limit***	***Upper Limit***	***Lower Weight***	***Upper Weight***	***Importance***	
Temperature *(^{o}C)*	maximize	30	40	1	1	3	
Time *(min)*	maximize	6	42	1	1	3	
Dosage *(mg/l)*	Is in range	1	5	1	1	3	
Initial Conc. *(ppm)*	Is in range	25	60	1	1	3	
Rem. Efficiency	maximize	72.41	88.45	1	1	3	
Solutions							
Number	***Temperature (^{o}C)***	***Time (min)***	***Dosage (mg/l)***	***Initial Conc. (ppm)***	***Removal Efficiency***	***Desirability***	***Remarks***
1	40.00	42.00	3.99	54.57	85.601	0.937	selected
2	40.00	42.00	4.13	53.36	85.5875	0.937	
3	40.00	42.00	3.76	54.77	85.5809	0.936	
4	40.00	42.00	3.70	51.23	85.539	0.935	
5	40.00	41.75	3.86	54.01	85.5737	0.934	
6	40.00	42.00	2.71	59.50	84.7896	0.917	
7	40.00	40.43	3.27	41.58	84.6159	0.899	
8	40.00	38.07	5.00	44.88	84.3036	0.871	
9	40.00	42.00	2.86	32.42	82.8683	0.867	
10	40.00	42.00	5.00	32.37	81.9359	0.841	

Table 6 shows the constraints and ten different solutions for the numerical approach. It was done for maximal temperature, time and removal efficiency. The first solution was selected by the software and that was adopted for this work.

Experimental validation of optimum point

The software used could only be relevant if the established points are validated. Accordingly, the present study seeks to validate the result obtained for RSM-based optimized process parameters. An independent run was carried out using a temperature of 40^{0}C, contact time of 42 min and an initial cyanide concentration of 47.39 mg/l. A maximum percentage removal of 85.27 achieved validated the design.

4.0 CONCLUSION

The copper impregnated adsorbent prepared from oil palm fiber ash appears to be a promising sustainable remediating medium for the removal of cyanide from simulated waste water. The adsorbent was characterized using XRF, XRD, SEM and FTIR. The response surface modelling was successfully combined with the four-level factorial, Box-Behnken design to determine the influence of contact time, temperature, initial concentration of cyanide and dosage of adsorbent. The maximum removal of cyanide of *85.27%* was obtained at *42 min contact time and temperature of 40^{o}C with 47.39 ppm, adsorbent*

dosage of 2.82 g. The second-order polynomial regression model was capable of interpreting the experimental data; it was shown that all the factors considered had significant effects on rate of cyanide removal. Increase in all these factors tends to enhance cyanide removal efficiency, an interactive combination between time-temperature and time-initial concentration seems to highly favour the removal of cyanide.

REFERENCES

Abbas, M. N., Abbas, F. S. and Ibrahim, S. A. (2014). Cyanide removal from wastewater by using banana peel. Journal of Asian Scientific Research, 4(5): 239-247.

Abdel-Aziz, M.H., Bassyouni, M., Gutub, S. A., El-Ashtoukhy, E. S. Z., Abdel-Hamid, S. M. S. and Sedahmed, G.H. (2016). Removal of Cyanide from Liquid Waste by Electrochemical Oxidation in a New Cell Design Employing a Graphite Anode. Chemical Engineering Communications, Vol. 203, Issue 8, Pages 1045-1052.

Abdullah, M.A., Nazir, M.S and Wahjoedi, B.A (2011): Development of value-added Biomaterials from Oil Palm Agro-wastes. 2nd International Conference on Biotechnology and Food Science. 32-35.

Abdullah, N., Sulaiman, F. and Gerhauser, H. (2011). Characterisation of Oil Palm Empty Fruit Bunches for Fuel Application. Journal of Physical Science, Vol. 22(1), 1–24, Penerbit Universiti Sains Malaysia.

Adams, M. D. (1994). Removal of cyanide from solution using activated carbon," Miner. Eng., 7(9), 1165-1177.

Adeoluwa, O. O .and Adeoye, G.O (2008). Potential of Oil Palm Empty Fruit Bunch (EFB) as Fertilizer in Oil Palm (*Elaeis guineensis* L. Jacq.) Nurseries. Poster at: Cultivating the Future Based on Science: 2nd Conference of the International Society of Organic Agriculture Research ISOFAR, Modena, Italy, June 18-20, 2008. Archieved at http:// orgprints.org/view/projects/conference.

Akcil, A. (2003). "Destruction of cyanide in gold mill effluents: biological versus chemical treatments," Biotechnol. Adv., 21(6), 501-511.

Anyanwu, C. N. (2013). Present and Prospective Energy Use Potentials of Selected Agricultural Wastes in Nigeria. *Journal of Renewable and Sustainable Energy*, 4-5.

Asadpour, R., Sapari, N.B., Isa, M.H. and Kakooei, S (2016). Acetylation of oil palm empty fruit bunch fiber as an adsorbent for removal of crude oil. Environ Sci Pollut Res Int. 23(12):11740-50.

ASTM D1102-84(2013). Standard Test Method for Ash in Wood, ASTM International, West Conshohocken, PA, 2013, www.astm.org.

ASTM E871-82(2013). Standard Test Method for Moisture Analysis of Particulate Wood Fuels, ASTM International, West Conshohocken, PA, 2013, www.astm.org.

ASTM E872-82(2013). Standard Test Method for Volatile Matter in the Analysis of Particulate Wood Fuels, ASTM International, West Conshohocken, PA, 2013, www.astm.org.

Bansal, R.C., Donnet, J.P. and Stoeckli, F. (1988). Active Carbon, Marcel Dekker, Inc., New York, NY.

Castro, J., Bonelli, P., Cerrella, E. and Cukierman, A. (2000). Phosphoric acid activation of agricultural residues and bagasse from sugar cane: influence of the experimental conditions on adsorption characteristics of activated carbons, Ind. Eng. Chem. Res; 39, 4166-4170.

Celik, H., Mordogan, H. and Ipekdogan, U. (1997). "A review of treatment methods for gold processing effluents containing cyanide," J. Chamber Mining Eng. Turkey, 36(1), 33-45.

Chua, S., Tan, C., Mirhosseini, H., Lai, O., Kamariah, L., and Baharin, B. (2009). Optimization of ultrasound extraction condition of phospholipids from palm-pressed fiber. J. Food Eng. 403–409.

Cooke, R.D., Richard, J.E. and Thompson, A.R. (1985). Nutritional aspect of cassava storage and processing. VIIth Symposium of the International Society for tropical Crops, Guadeloupe, July 1985. Pp 645-648.

Dash, R. R., Balomajumder, C. and Kumar, A. (2009). "Treatment of cyanide bearing water/Wastewater by plain and Biological Activated Carbon," Ind. Eng. Chem. Res., 48(7), 3619-3627.

Depci, T. (2011). Comparison of activated carbon and iron impregnated activated carbon derived. *Chemical Engineering Journal*, 4.

Dumestre, A., Chone, T., Portal, M.J., Gerard, M. and Berthelin, J. (1997). Cyanide degradation under alkaline conditions by a strain of Fusarium solani isolated from contaminated soil. Appl Environ. Microbiol. 66(7):2729-2734.

Ebbs, S. (2004). Biological degradation of cyanide compounds. Curr. Opinion in Biotech. *15*:231-236.

Fleming, C.A. and Cromberge, G. (1984). The Extraction of Gold from Cyanide Solutions by Strong and Weak-Base Anion-Exchange Resins, J. S. Afr. Inst. Min. Metall., 84:125-138.

Herawan, S.G., Hadi, M. S., Ayob, Md. R. and Putra, A. (2013). Characterization of Activated Carbons from Oil-Palm Shell by CO_2 Activation with no Holding Carbonization Temperature. The Scientific World Journal.

Kalavathy, M.H., Regupathi, I., Pillai, M.G. and Miranda, L.R. (2009). Modelling, analysis and optimization of adsorption parameters for H_3PO_4 activated rubber wood sawdust using response surface methodology (RSM). Colloids Surf B 70(1):35–45

Megat-Johari, M.A., Zeyad, A.M., Muhamad Bunnori, N. and Ariffin, K.S. (2012). Engineering and transport properties of high-strength green concrete containing high volume of ultrafine palm oil fuel ash. Construction and Building Materials. Vol. 30. 281-288.Elsevier.

Mert, B. K., Sivrioğlu, O., Yonar, T and Özçiftçi, S. (2014). Treatment of Jewelry Manufacturing Effluent Containing Cyanide Using Ozone-Based Photochemical Advanced Oxidation Processes. Ozone: Science & Engineering, The Journal of the International Ozone Association Vol. 36, Issue 2, pages 196-205.

Muir, D.M., Aziz, M. and Hoecker, W. (1988). Cyanide Losses under CIP Conditions and Effect of Carbon on Cyanide Oxidation, In: Proc. Int. Hydromet. Conf., Beijing, China.

Myers, R.H and Montgomery, D.C., (1995). Response surface methodology: Process and product optimization using designed experiments, Vol. 22. John Wiley and Sons, Inc. New York.

Ohimain, E., Izah, S and Obieze, F (2013). Material-mass balance of smallholder oil palm processing in the Niger Delta, Nigeria. Advance J Food Sci Technol, 5(3): 289-294.

Oliver, T. M., Jugoslav, K., Aleksandar, P., and Nikola, D. (2005). "Synthetic activated carbons for the removal of hydrogen cyanide from air," Chem. Eng. Process., 44(11), 1181-1187.

Osuntokun, B.O. (1994). Chronic cyanide intoxication of dietary origin and a degenerative neuropathy in Nigerians. *Acta Hort. 375*:311-321.

Parveen, F.R., Rajeev, P.S., Ibrahim, M.H., and Esa, N. (2010). Review of current palm oil mill effluent treatment: Vermicomposting as an austainable practise. World Applied Sciences Journal, 11(1), 70-81.

Paul, G. (2004). Design of Experiments with MINITAB, Mathews, Amer Society for Quality.

Poku, K. (2002). Small-Scale Palm Oil Processing in Africa.FAO Agriculture Services Bulletin 148, Food and Agricultural Organization of the United Nations, Rome, Italy.

Prasertsan, S. and Prasertsan, P (1996). Biomass residues from palm oil mills in Thailand: an overview on quantity and potential usage. Biomass Bioenergy, perspective.11(5): 87-395.

Pueyo N., Miguel, N., Ovelleiro, J.L and Ormad, M.P (2016). Limitations of the removal of cyanide from coking wastewater by ozonation and by the hydrogen peroxide-ozone process. Water Sci Technol. 74(2):482-90. doi: 10.2166/wst.2016.227.

Refaat Abdel-Fattah, Y. (2002). Optimization of thermostable lipase production from a thermophilic Geobacillus sp. using Box-Behnken experimental design, Biotechnology Letters 24: 1217–1222.

Ridzuan, R., Khan, Md. M. R.., Rosli, M. Y., Huei, R. O., Halim, R.M., Aziz, A. A.., Zawawi, I and Zainal, N. H. (2014). *In-Situ* Impregnation of Copper Nanoparticles on Palm Empty Fruit Bunch Powder. Advances in Nanoparticles, 2014, 3, 65-71. Published Online August 2014 in SciRes. http://www.scirp.org/journal/anp

Rincon S. L. and Gomez A. (2012). Comparative behaviour of agricultural biomass residues during thermo chemical processing, Global NEST Journal, vol. 14, no. 2, pp. 111–117.

Saxena, S., Prasad, M., Amritphale, S. S., and Chandra, N. (2001). Adsorption of cyanide from aqueous solutions at pyrophyllite surface, Sep. Puri. Technol., 24(1-2),263-270.

Shariff, A., N. S. M. Aziz and N. Abdullah (2014). Slow Pyrolysis of Oil Palm Empty Fruit Bunches for Biochar Production and Characterisation. Journal of Physical Science, Vol. 25(2), 97–112. Penerbit Universiti Sains Malaysia, 2014

Shinoj, S., Visvanathan, R., Panigrahi, S., and Kochubabu, M. (2011). Oil palm fiber (OPF) and its composite. *A review. Ind. Crop. Prod.*, 33, 7–22.

Singh, R.P., Hakimi, I.M. and Esa, N. (2010). Composting of waste from palm oil mill: A College, London. 190 Rajah Rasiah. Sustainable waste management practice. Review in Environmental Science and Biotechnology, DOI: 10.1007/s11157-010-9199-2.

Szabo, E.A., Jansson, E., Miles, D., Hambridge, T., Stanley, G., Baines, J. and Brent, P. (2010). Chapter 24 – Responding to Incidents of Low Level Chemical Contamination in Food. Ensuring Global Food Safety. Exploring Global Harmonization. Pages 411–437.

Tangchirapat, W. and Jaturapitakkul, C. (2010). Strength, drying shrinkage, and water permeability of concrete incorporating ground palm oil fuel ash. *Cement and Concrete Composites*, *32*(10), 767-774.

Whittle, L. (1992). The Piloting of Vitrokele for Cyanide Recovery and Waste Management at Two Canadian Gold Mines, Randol Gold Forum, Randol Int. Ltd., Golden, CO.

Yeddou, A.R., Nadjemi, B., Halet, F., Ould-Dris, A. and Capart, R. (2010). Removal of cyanide in aqueous solution by oxidation with hydrogen peroxide in presence of activated carbon prepared from olive stones. Minerals Engineering, Volume 23, Issue 1, Pages 32-39

Yetilmezsoy, K., Demirel, S., and Vanderbei, R.J. (2009). Response surface modeling of Pb(II) removal from aqueous solution by Pistacia vera L.: Box–Behnken experimental design. J Hazard Mater, 171(1–3):551–562.

Yojiro, K. and Ishizaki, A. (1990). Chemical Composition of Palm Fiber and Its Feasibility as Cellulosic Raw Material for Sugar Production, Agricultural and Biological Chemistry, 54:5, 1183-1187.

Young, C. A. and Jordan, T. S. (1995). Cyanide remediation: current and past technologies. Proceedings of the 10th Annual Conference on Hazardous Waste Research, Great Plains/Rocky Mountain Hazardous Substances Research Center, Kansas State University, Kansas:104-129.

Zarina, Y., Mustafa-Al Bakri, A.M., Kamarudin1, H I. Khairul Nizarand A. and Rafiza, R. (2013). Review on the various ash from palm oil waste as geopolymer material. Rev.Adv. Mater. Sci. 34, 37-43

Zhang, J. and Hendrix, J.L. (1991). Attenuation of Cyanide in Soils, In: D.R. Gaskell (Ed.), EPD Congress '91, TMS, Warrendale, PA, pp. 677-686